

Synthesis and Characterization of Volatile, Thermally Stable, Reactive Transition Metal Amidinates

Booyong S. Lim, Antti Rahtu, Jin-Seong Park, and Roy G. Gordon*

Department of Chemistry and Chemical Biology, Harvard University,
Cambridge, Massachusetts 02138

Received May 19, 2003

A series of homoleptic metal amidinates of the general type $[M(R-R'AMD)_n]_x$ ($R = \textit{i}Pr, \textit{t}Bu, R' = Me, \textit{t}Bu$) has been prepared and structurally characterized for the transition metals Ti, V, Mn, Fe, Co, Ni, Cu, Ag, and La. In oxidation state 3, monomeric structures were found for the metals Ti(III), V(III), and La(III). Bridging structures were observed for the metals in oxidation state 1. Cu(I) and Ag(I) are held in bridged dimers, and Ag(I) also formed a trimer that cocrystallized with the dimer. Metals in oxidation state 2 occurred in either monomeric or dimeric form. Metals with smaller ionic radii (Co, Ni) were monomeric. Larger metals (Fe, Mn) gave monomeric structures only with the bulkier *tert*-butyl-substituted amidinates, while the less bulky isopropyl-substituted amidinates formed dimers. The new compounds were found to have properties well-suited for use as precursors for atomic layer deposition (ALD) of thin films. They have high volatility, high thermal stability, and high and properly self-limited reactivity with molecular hydrogen, depositing pure metals, or water vapor, depositing metal oxides.

Introduction

Highly conformal thin films of transition metals and metal oxides are needed in a variety of technological applications including microelectronics, magnetic information storage, and catalysis. For example, transition metal thin films can be used as adhesion/seed layers in copper interconnects¹ and as magnetoresistive multilayers in advanced designs of magnetic random access memory devices.² There is also considerable interest in lanthanide oxides such as La_2O_3 due to their potential application as an insulator for memory and logic devices.³

Atomic layer deposition (ALD) is a modified chemical vapor deposition (CVD) process that can provide very uniform and conformal films needed for these applications. In ALD, films are grown by alternating exposures of a heated substrate to vapors of two complementary chemical precursors. The main difference between ALD and CVD is that, in ALD, the surface reactions are self-limited. ALD processes

have been discovered for many metal oxides, nitrides, fluorides, and sulfides and a few pure metals.⁴ Applications of ALD to the production of thin films have recently grown rapidly.⁵ Magnetic disk drives now incorporate an ALD layer,⁶ and ALD insulating layers are used in microelectronic memory chips.⁷ Wider use of ALD is, however, hindered by the scarcity of suitable precursors. In particular, no fully satisfactory precursors are known for ALD of the later first-row transition metals (Mn, Fe, Co, Ni, Cu), or for the lanthanide metals.

For deposition of films by ALD, precursors need to be designed in such a way that the compounds are highly reactive toward the surfaces of substrates and also to the surface prepared by a complementary precursor such as H_2O , NH_3 , or H_2 . Such precursors also must be volatile and must be thermally stable at growth temperatures, and preferably the reaction byproducts should be nonreactive and non-corrosive. ALD precursor chemistry has been dominated by halides, alkoxides, β -diketonates, alkyls, cyclopentadienyl derivatives, and heteroleptic compounds involving mixtures

* Author to whom correspondence should be addressed. E-mail: Gordon@chemistry.harvard.edu.

- (1) *International Technology Roadmap for Semiconductors 2002 Update*; Semiconductor Industry Association, 2002. Published on the Internet at <http://public.itrs.net/Files/2002Update/Home.pdf>, Interconnect Chapter.
- (2) Durlam, M.; Chen, E. Y.; Tehrani, S. N.; Slaughter, J. M.; Kerszykowski, G.; Kyler, K. W. *US Patent* 6,211,090 **2001**.
- (3) Copel, M.; Cartier, E.; Ross, F. M. *Appl. Phys. Lett.* **2001**, *78*, 1607–1609.

- (4) Ritala, M.; Leskelä, M. In *Handbook of Thin Film Materials*; Nalwa, H. S., Ed.; Academic Press: New York, 2001; Vol. 1, pp 103–159.
- (5) Suntola, T.; Simpson, M., Eds. *Atomic Layer Epitaxy*; Blackie and Sons Ltd.: Glasgow, 1990.
- (6) Xiong, W.; Gong, H.; Park, C.-M.; Zhang, J.; Lam, A.; Huai, Y. *MMM Conf.* **2001**, Session HP-03.
- (7) Seidel, T.; Londergan, A.; Winkler, J.; Liu, X.; Ramanathan, S. *Solid State Technol.* **2003**, *46*, 67–68.

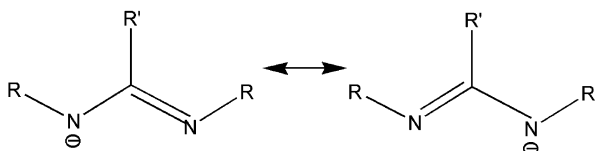


Figure 1. Bidentate chelating N,N' -dialkyl-2-alkyl-amidinate ligand.

of these ligands.⁸ Recently, dialkylamido compounds $[\text{Zr}(\text{NR}_2)_4]$, $[\text{Hf}(\text{NR}_2)_4]$, and mixed dialkylamido/alkylimido compounds $[\text{W}(\text{NR}_2)_2(\text{N}'\text{Bu})_2]$ have been successfully utilized for the ALD of thin films of zirconium and hafnium oxides⁹ and tungsten nitride.¹⁰ Because these amide-type precursors do not have M–C bonds, carbon incorporation in the resulting films was found to be minimal, and the low M–N bond strengths as compared to the M–Cl and M–O bonds allowed deposition at relatively low temperatures. These amide derivatives produce no corrosive byproducts, unlike metal halides.

The most extensively studied homoleptic amido metal compounds are those with bis(trimethylsilyl)amide (TMS) ligand. This bulky TMS group has been used to stabilize especially low coordination numbers (2, 3) and oxidation states (1, 2, 3) throughout the periodic table.^{11–14} Although this class of metal compounds generally provided high chemical reactivity, silicon contamination in films and low thermal stability have often limited their use in ALD.¹⁵ Volatile homoleptic amido metal compounds containing moieties other than the TMS group are rare, with most examples from the group 4–6 metals. It is notable that most volatile homoleptic dialkylamido metal compounds are those with high oxidation states of 4 or more. Dialkylamides of transition metals with low oxidation states of 1–3 are not volatile. For example, tetrameric $[\text{Cu}(\text{NR}_2)_4]$ ($\text{R} = \text{Me}, \text{Et}, n\text{Bu}, \text{Cy}$) decomposed before sublimation, which prevents their use as precursors for vapor deposition.¹⁶

N,N' -Dialkyl-2-alkyl-amidates ($\text{R-R}'\text{AMD}$) are alternatives to alkylamides (Figure 1). The amidinate ligand can be tuned by substitution of the R and R' groups to be bulky enough to limit oligomerization and hence increase the volatility of amidinate compounds of metals in low oxidation states. The bidentate chelating effect should increase the thermal stability of resulting metal compounds. While numerous metal compounds with amidinate ligands can be found in the literature,^{17–23} volatility and thermal stability

have been studied for only three magnesium amidates, $[\text{Mg}(\text{R-MeAMD})_2]_x$ ($x = 1, \text{R} = t\text{Bu}; x = 2, \text{R} = i\text{Pr}, \text{Et}$).²⁴

We demonstrate here that bidentate amidinate ligands provide volatile, thermally stable, homoleptic compounds with a wide range of transition metals and lanthanum with oxidation states of 1 (Cu, Ag), 2 (Mn, Fe, Co, Ni), and 3 (Ti, V, La). The compounds $[\text{M}(\text{R-R}'\text{AMD})_3]$ ($\text{M} = \text{Ti}, \text{V}, \text{La}$), $[\text{M}(\text{R-MeAMD})_2]_x$ ($\text{M} = \text{Mn}, \text{Fe}, \text{Co}, \text{Ni}, x = 1, 2$), and $[\text{M}(\text{R-MeAMD})]_x$ ($\text{M} = \text{Cu}, \text{Ag}, x = 2, 3$) ($\text{R} = i\text{Pr}, t\text{Bu}, \text{R}' = \text{Me}, t\text{Bu}$) were characterized by X-ray crystallography, elemental analysis, NMR, physical characteristics (color, melting point, vapor pressure), thermal stability, and chemical reactivity. All of these metal amidates are volatile. Among them, manganese, iron, cobalt, nickel, copper, and lanthanum compounds were tested for thin film deposition, and were found thermally stable and reactive enough to be used as vapor sources for the ALD of pure transition metal films of Fe, Co, Ni, and Cu and of metal oxides La_2O_3 , FeO , MnO , and CoO .²⁵

Experimental Section

Preparation of Compounds. All reactions and manipulations were conducted under a pure nitrogen atmosphere using either an inert atmosphere box or standard Schlenk techniques. Tetrahydrofuran (THF), ether, and hexanes were dried using an Innovative Technology solvent purification system and stored over 4 Å molecular sieves. Methylolithium, *tert*-butyllithium, 1,3-diisopropylcarbodiimide, 1,3-di-*tert*-butylcarbodiimide, TiCl_3 , VCl_3 , MnCl_2 , FeCl_2 , CoCl_2 , NiCl_2 , CuBr , and AgCl (Aldrich) were used as received. $\text{LaCl}_3(\text{THF})_2$ was prepared as described in the literature.²⁶

Copper (N,N' -Diisopropylacetamidate) ($[\text{Cu}(i\text{Pr-MeAMD})_2]$) (7). A solution of methylolithium (1.6 M in Et_2O , 34 mL, 0.054 mol) in Et_2O was added dropwise to a solution of 1,3-diisopropylcarbodiimide (6.9 g, 0.055 mol) in 100 mL of Et_2O at -30°C . The mixture was warmed to room temperature and stirred for 4 h. This colorless resultant solution was then added to a solution of copper bromide (7.8 g, 0.054 mol) in 50 mL of Et_2O . The reaction mixture was stirred for 12 h under the exclusion of light. All volatiles were then removed under reduced pressure, and the resulting solid was extracted with hexanes (100 mL). The hexane extract was filtered through a pad of Celite on a glass frit to afford a pale yellow solution. Concentration of the filtrate and its cooling to -30°C afforded colorless crystals. Subsequent sublimation afforded pure white products (70%). Sublimation: 70°C at 50 mTorr. Mp: 147°C . $^1\text{H NMR}$ (C_6D_6 , 25°C): 1.16 (d, 12H), 1.65 (s, 3H), 3.40 (m, 2H). Anal. Calcd for $\text{C}_{16}\text{H}_{34}\text{N}_4\text{Cu}_2$: C, 46.92; H, 8.37; N, 13.68. Found: C, 46.95; H, 8.20; N, 13.78.

- (8) Leskelä, M.; Ritala, M. *Thin Solid Films* **2002**, *409*, 138–146.
 (9) Hausmann, D. M.; Kim, E.; Becker, J.; Gordon, R. G. *Chem. Mater.* **2002**, *14*, 4350–4358.
 (10) Becker, J. S.; Gordon, R. G. *Appl. Phys. Lett.* **2003**, *82*, 2239–2241.
 (11) Bradley, D. C.; Ghotra, J. S.; Hart, F. A. *J. Chem. Soc., Dalton Trans.* **1973**, 1021.
 (12) Olmstead, M. M.; Power, P. P.; Shoner, S. C. *Inorg. Chem.* **1991**, *30*, 2547 and references therein.
 (13) Hitchcock, P. B.; Lappert, M. F.; Pierssens, L. J.-M. *Chem. Commun.* **1996**, 1189.
 (14) Lappert, M. F., Ed. *Metals and Metalloid Amides*; John Wiley & Sons: New York, 1980; p 465.
 (15) Kim, D.-H.; Gordon, R. G. Unpublished results.
 (16) (a) Tsuda, T.; Watanabe, K.; Miyata, K.; Yamamoto, H.; Saegusa, T. *Inorg. Chem.* **1981**, *20*, 2728–2730. (b) Hope, H.; Power, P. P. *Inorg. Chem.* **1984**, *23*, 936–937.
 (17) Edelmann, F. T.; Freckmann, D. M. M.; Schumann, H. *Chem. Rev.* **2002**, *102*, 1851–1896.

- (18) Cotton, F. A.; Daniels, L. M.; Murillo, C. A. *Inorg. Chem.* **1993**, *32*, 2881–2885 and references therein.
 (19) Cotton, F. A.; Daniels, L. M.; Matonic, J. H.; Murillo, C. A. *Inorg. Chim. Acta* **1997**, *256*, 277–282.
 (20) Cotton, F. A.; Daniels, L. M.; Feng, X.; Maloney, D.; Matonic, J. H.; Murillo, C. A. *Inorg. Chim. Acta* **1997**, *256*, 291–301.
 (21) Cotton, F. A.; Feng, X.; Matusz, M.; Poli, R. *J. Am. Chem. Soc.* **1988**, *110*, 7077–7083.
 (22) Luo, Y.; Yao, Y.; Shen, Q.; Sun, J.; Weng, L. *J. Organomet. Chem.* **2002**, *662*, 144–149.
 (23) Vendemiati, B.; Prini, G.; Meetsma, A.; Hessen, B.; Teuben, J. H.; Traverso, O. *Eur. J. Inorg. Chem.* **2002**, 707–711.
 (24) Sadique, A. R.; Heeg, M. J.; Winter, C. H. *Inorg. Chem.* **2001**, *40*, 6349–6355.
 (25) Lim, B. S.; Rahtu, A.; Gordon, R. G. *Nature Materials*, in press.
 (26) Deacon, G. B.; Feng, T.; Nickel, S.; Skelton, B. W.; White, A. H. *J. Chem. Soc., Chem. Commun.* **1993**, 1328.

Silver (*N,N'*-Diisopropylacetamidinate) ([Ag(ⁱPr-MeAMD)]_x (*x* = 2, **8a; *x* = 3, **8b**)).** These compounds were prepared in the same manner as described for [Cu(ⁱPr-MeAMD)], and obtained as a 1:1 mixture of dimer and trimer. The product was isolated as colorless crystals (90%). Sublimation: 80 °C at 40 mTorr. Mp: 95 °C. ¹H NMR (C₆D₆, 25 °C): 1.10 (d, dimer), 1.21 (d, trimer), 1.74 (s, trimer), 1.76 (s, dimer), 3.52 (m, peaks for dimer and trimer are not well resolved.) Anal. Calcd for [C₈H₁₇N₂Ag]_x: C, 38.57; H, 6.88; N, 11.25. Found: C, 38.62; H, 6.76; N, 11.34.

Cobalt Bis(*N,N'*-Diisopropylacetamidinate) ([Co(ⁱPr-MeAMD)₂]) (5a**).** This compound was obtained in a similar manner as described for [Cu(ⁱPr-MeAMD)], but with Et₂O/THF (1:1, v/v) as solvents. Recrystallization in hexanes at -30 °C gave dark green crystals as product (77%). ¹H NMR (C₆D₆, 25 °C): -70.56 (br, 12H), 310.53 (br, 3H), 326.34 (br, 2H). Sublimation: 40 °C at 50 mTorr. Mp: 84 °C. Anal. Calcd for C₁₆H₃₄N₄Co: C, 56.29; H, 10.04; N, 16.41. Found: C, 54.31; H, 9.69; N, 15.95.

All the following compounds have been synthesized in the same way as [Co(ⁱPr-AMD)₂] unless described otherwise.

Cobalt bis(*N,N'*-di-*tert*-butylacetamidinate) ([Co(^tBu-MeAMD)₂]) (5b**):** dark blue crystals (84%). ¹H NMR (C₆D₆, 25 °C): -28.86 (br, 18H), 312.21 (br, 3H). Sublimation: 45 °C at 50 mTorr. Mp: 90 °C. Anal. Calcd for C₂₀H₄₂N₄Co: C, 60.43; H, 10.65; N, 14.09. Found: C, 58.86; H, 10.33; N, 14.28.

Iron bis(*N,N'*-diisopropylacetamidinate) ([Fe₂(ⁱPr-MeAMD)₂-(^η2-ⁱPr-MeAMD)₂]) (4a**):** yellow-green crystals (75%). ¹H NMR (C₆D₆, 25 °C): 5.12 (br, 12H), 130.66 (br, 3H), 177.44 (br, 2H); unassignable broad peaks (5–10% intensity of that at 5.12 peak) at -10.30, -6.75, -2.31, 22.10, 110.27, 139.39, 199.64, and 217.03 were also observed. Sublimation: 70 °C at 50 mTorr. Mp: 110 °C. Anal. Calcd for C₃₂H₆₈N₈Fe₂: C, 56.80; H, 10.13; N, 16.56. Found: C, 55.24; H, 10.05; N, 16.17. Complexity in solution (*p*-xylene): 2.0(2).

Iron bis(*N,N'*-di-*tert*-butylacetamidinate) ([Fe(^tBu-MeAMD)₂]) (4b**):** white crystals (77%). ¹H NMR (C₆D₆, 25 °C): 15.78 (br, 18H), 154.46 (br, 3H). Sublimation: 55 °C at 60 mTorr. Mp: 107 °C. Anal. Calcd for C₂₀H₄₂N₄Fe: C, 60.90; H, 10.73; N, 14.20. Found: C, 59.55; H, 10.77; N, 13.86.

Nickel bis(*N,N'*-diisopropylacetamidinate) ([Ni(ⁱPr-MeAMD)₂]) (6**).** This compound was prepared in the manner of **7** but with refluxing the reaction mixtures at 60 °C overnight. Brown crystals (49%). Sublimation: 35 °C at 70 mTorr. Mp: 69 °C. ¹H NMR (C₆D₆, 25 °C): -5.39 (br, 12H), 30.9 (br, 3H), 81.16 (br, 2H). Anal. Calcd. for C₁₆H₃₄N₄Ni: C, 56.34; H, 10.05; N, 16.42. Found: C, 55.22; H, 10.19; N, 16.12. Complexity in solution (*p*-xylene): 1.0(2).

Manganese bis(*N,N'*-diisopropylacetamidinate) ([Mn₂(ⁱPr-MeAMD)₂(^η2-ⁱPr-MeAMD)₂]) (3a**):** pale yellow crystals (79%). Sublimation: 65 °C at 50 mTorr. Mp: 148 °C. Anal. Calcd for C₃₂H₆₈N₈Mn₂: C, 56.96; H, 10.16; N, 16.61. Found: C, 57.33; H, 9.58; N, 16.19.

Manganese bis(*N,N'*-di-*tert*-butylacetamidinate) ([Mn(^tBu-MeAMD)₂]) (3b**):** pale yellow crystals (87%). Sublimation: 55 °C at 60 mTorr. Mp: 100 °C. Anal. Calcd for C₂₀H₄₂N₄Mn: C, 61.04; H, 10.76; N, 14.24. Found: C, 60.53; H, 11.31; N, 14.03.

Titanium tris(*N,N'*-diisopropylacetamidinate) ([Ti(ⁱPr-MeAMD)₃]) (1**):** brown crystals (70%). Sublimation: 70 °C at 50 mTorr. ¹H NMR (C₆D₆, 25 °C): -12.3 (br, 3H), 0.77 (br, 6H), 1.46 (br, 6H), 40.7 (br, 2H). Anal. Calcd. for C₂₄H₅₁N₆Ti: C, 61.13; H, 10.90; N, 17.82. Found: C, 60.22; H, 10.35; N, 17.14.

Vanadium tris(*N,N'*-diisopropylacetamidinate) ([V(ⁱPr-MeAMD)₃]) (2**):** red-brown powder (80%). Sublimation: 70 °C at 45 mTorr. ¹H NMR (C₆D₆, 25 °C): -39.1 (br, 3H), 0.41 (br, 6H),

3.26 (br, 6H), 96.3 (br, 2H). Anal. Calcd. for C₂₄H₅₁N₆V: C, 60.73; H, 10.83; N, 17.71. Found: C, 61.45; H, 11.17; N, 17.78.

Lanthanum tris(*N,N'*-diisopropylacetamidinate) ([La(ⁱPr-MeAMD)₃]) (9a**):** following a similar procedure as described above for [Co(ⁱPr-MeAMD)₂], but using LaCl₃(THF)₂,²⁶ off-white solids were obtained as a product by sublimation of the crude solid materials (77%). Sublimation: 80 °C at 40 mTorr. ¹H NMR (C₆D₆, 25 °C): 1.20 (d, 12H), 1.67 (s, 3H), 3.46 (m, 2H). Anal. Calcd for C₂₄H₅₁N₆La: C, 51.24; H, 9.14; N, 14.94. Found: C, 51.23; H, 8.22; N, 14.57.

Lanthanum tris(*N,N'*-diisopropyl-2-*tert*-butylamidinate) ([La(ⁱPr-^tBuAMD)₃]-¹/₂C₆H₁₂) (9b**):** colorless crystals (80%). Sublimation: 120 °C at 50 mTorr. Mp: 140 °C. ¹H NMR (C₆D₆, 25 °C): 1.33 (br, 21H), 4.26 (m, 2H); the methyl resonance of isopropyl groups and *tert*-butyl group of the ligand was not resolved. Anal. Calcd for C₃₃H₇₅N₆La: C, 57.04; H, 10.88; N, 12.09. Found: C, 58.50; H, 10.19; N, 11.89.

X-ray Structure Determinations. Compounds [V(ⁱPr-MeAMD)₃] (**2**), [Fe₂(ⁱPr-MeAMD)₂(^η2-ⁱPr-MeAMD)₂] (**4a**), [Fe(^tBu-MeAMD)₂] (**4b**), [Co(ⁱPr-MeAMD)₂] (**5a**), [Cu(ⁱPr-MeAMD)₂] (**7**), [Ag(ⁱPr-MeAMD)]_x (**8a**, **8b**), and [La(ⁱPr-^tBuAMD)₃] (**9b**) were structurally characterized by X-ray crystallography. Crystals were grown by standing saturated hexane solutions at -30 °C overnight. Diffraction data were obtained with a Siemens (Bruker) SMART CCD area detector system using ω scans of 0.3°/frames, and 30-s frames such that 1271 frames were collected for a hemisphere of data. The first 50 frames were re-collected at the end of the data collection to monitor for crystal decay; no significant decay was observed. Cell parameters were determined using SMART software. Data reductions were performed with SAINT software, which corrects for Lorenz polarization and decay. Absorption corrections were applied using SADABS. Space groups were assigned by analysis of symmetry and observed systematic absences determined by the program XPREP and by successful refinement of the structure. All structures were solved by direct methods with SHELXS and subsequently refined against all data by the standard technique of full-matrix least squares on *F*² (SHELXL-97).

The asymmetric units contain one-half (**4a**, **4b**, **5a**, **8a**), one (**8b**, **9b**), two of one-half (**7**), or one-third (**2**) formula weights. The structure of **2** was highly disordered over four different positions and refined accordingly, and also refined with a chiral twin treatment with BASF = 0.59. Isopropyl groups in **5a** and **9b** were disordered over two positions and were refined accordingly. All non-hydrogen atoms except for the solvated hexane molecule found in **9b** were described anisotropically. In the final stages of refinement, hydrogen atoms were added at idealized positions and refined as riding atoms with a uniform value of *U*_{iso}. Crystal data and final agreement factors are listed in Table 1.

Other Physical Measurements. Elemental analysis was performed by Desert Analytics Laboratory, Tucson, AZ. ¹H NMR spectra were recorded with a Bruker AM-500 spectrometer. Melting points were obtained in sealed capillaries. Molecular weight determinations of compounds in solution were performed using 3.0–3.5 g of recrystallized *p*-xylene and 0.20–0.30 g of compound. The temperature was recorded electronically from a thermocouple every 10 s for at least 2 min, and the measurements were repeated at least three times to ensure reproducibility. Thermal gravimetric analysis (TGA) and differential scanning calorimetry (DSC) were done in a Netzsch STA 449C operated inside a drybox. Samples (10–20 mg) were loaded into open aluminum crucibles. Measurements were carried out at atmospheric pressure in a carrier gas of purified N₂ at a temperature ramp rate of 10 K/min.

Table 1. Crystallographic Data^a for Compounds **2**, **4a**, **4b**, **5a**, **7**, **8a**, **8b**, and **9b**

	2	4a	4b	5a	7	8	9b ^{1/2} C ₆ H ₁₂
formula	C ₂₄ H ₅₁ N ₆ V	C ₃₂ H ₆₈ Fe ₂ N ₈	C ₂₀ H ₄₂ FeN ₄	C ₁₆ H ₃₄ CoN ₄	C ₁₆ H ₃₄ Cu ₂ N ₄	C ₃₂ H ₆₈ Ag ₄ N ₈	C ₃₆ H ₇₅ LaN ₆
fw	474.65	676.64	394.43	341.41	409.56	996.44	730.94
cryst syst	hexagonal	monoclinic	tetragonal	monoclinic	monoclinic	monoclinic	monoclinic
space group	<i>R</i> 3 <i>m</i>	<i>C</i> 2/ <i>c</i>	<i>Aba</i> 2	<i>C</i> 2/ <i>c</i>	<i>C</i> 2/ <i>c</i>	<i>C</i> 2(1)/ <i>c</i>	<i>C</i> 2/ <i>c</i>
<i>Z</i>	3	4	4	4	8	4	8
<i>a</i> , Å	16.205(3)	23.290(6)	14.687(2)	14.109(2)	28.85(6)	24.942(3)	38.22(2)
<i>b</i> , Å	16.205(3)	9.629(2)	13.942(2)	9.455(2)	11.09(3)	9.924(1)	11.840(6)
<i>c</i> , Å	9.355(2)	18.194(4)	11.756(1)	15.476(2)	18.88(4)	17.122(2)	21.01(1)
β , deg		110.804(4)		100.875(3)	133.20(2)	104.739(2)	118.604(6)
<i>V</i> , Å ³	2127.6(7)	3814(2)	2407.3(5)	2027.3(5)	3946(2)	4098.7(9)	8347(8)
<i>d</i> _{calc} , g/cm ³	1.111	1.178	1.088	1.119	1.379	1.615	1.163
μ , mm ⁻¹	0.370	0.791	0.635	0.847	2.158	1.913	1.052
θ range, deg	2.51–28.23	1.87–22.50	2.77–28.31	2.80–28.27	2.13–22.49	0.84–28.28	1.82–28.41
GOF (<i>F</i> ²)	1.050	1.089	1.057	1.047	1.040	1.058	1.053
<i>R</i> ₁ ^b (<i>wR</i> ₂ ^c), %	4.24(11.30)	2.88(8.65)	2.94(8.26)	3.83(10.84)	4.29(10.54)	3.76(9.85)	3.19(0.13)

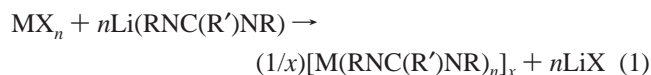
^a Obtained with graphite monochromated Mo K α ($\lambda = 0.71073$ Å) radiation. ^b $R_1 = \sum||F_o| - |F_c||/\sum|F_o|$. ^c $wR_2 = \{\sum[w(F_o^2 - F_c^2)^2]\}/\{\sum[w(F_o^2)^2]\}^{1/2}$.

Table 2. Physical Properties of Amidinato Metal Compounds **1–9**

compound	vapor pressure (°C/Torr)	mp (°C)	color
[Ti(ⁱ Pr-MeAMD) ₃], 1	70/0.05		brown
[V(ⁱ Pr-MeAMD) ₃], 2	70/0.05		red-brown
[Mn(ⁱ Pr-MeAMD) ₂] ₂ , 3a	65/0.05	148	pale yellow
[Mn(^t Bu-MeAMD) ₂] ₂ , 3b	55/0.06	100	pale yellow
[Fe(ⁱ Pr-MeAMD) ₂] ₂ , 4a	70/0.05	110	yellow-green
[Fe(^t Bu-MeAMD) ₂] ₂ , 4b	55/0.06	107	white
[Co(ⁱ Pr-MeAMD) ₂], 5a	40/0.05	84	dark green
[Co(^t Bu-MeAMD) ₂], 5b	45/0.05	90	dark blue
[Ni(ⁱ Pr-MeAMD) ₂], 6	35/0.07	69	brown
[Cu(ⁱ Pr-MeAMD) ₂], 7	70/0.05	147	white
[Ag(ⁱ Pr-MeAMD)] _x , 8a,b	80/0.04	95	white
[La(ⁱ Pr-MeAMD) ₃], 9a	80/0.04		white
[La(ⁱ Pr- ^t BuAMD) ₃], 9b	120/0.05	140	white

Results and Discussion

Synthesis and Structures of Compounds. All neutral metal amidinate compounds listed in Table 2 were synthesized by the metathesis reactions of a metal halide with corresponding equivalents of lithium amidinates (*N,N'*-diisopropylacetamidinate (ⁱPr-MeAMD), *N,N'*-di-*tert*-butylacetamidinate (^tBu-MeAMD), and *N,N'*-diisopropyl-2-*tert*-butylamidinate (ⁱPr-^tBuAMD)) in Et₂O or Et₂O/THF as described in reaction 1.



Lithium amidinates were prepared in situ from the corresponding carbodiimide and alkyllithium and not isolated; the metal complexes are depicted in Scheme 1. The reactions went to completion after stirring at room temperature overnight, except for the reaction for Ni(II) compound **6**, which was refluxed in THF/Et₂O (1:1, v/v) overnight. Compounds **1–9** are all solids at room temperature, and their physical properties are summarized in Table 2.

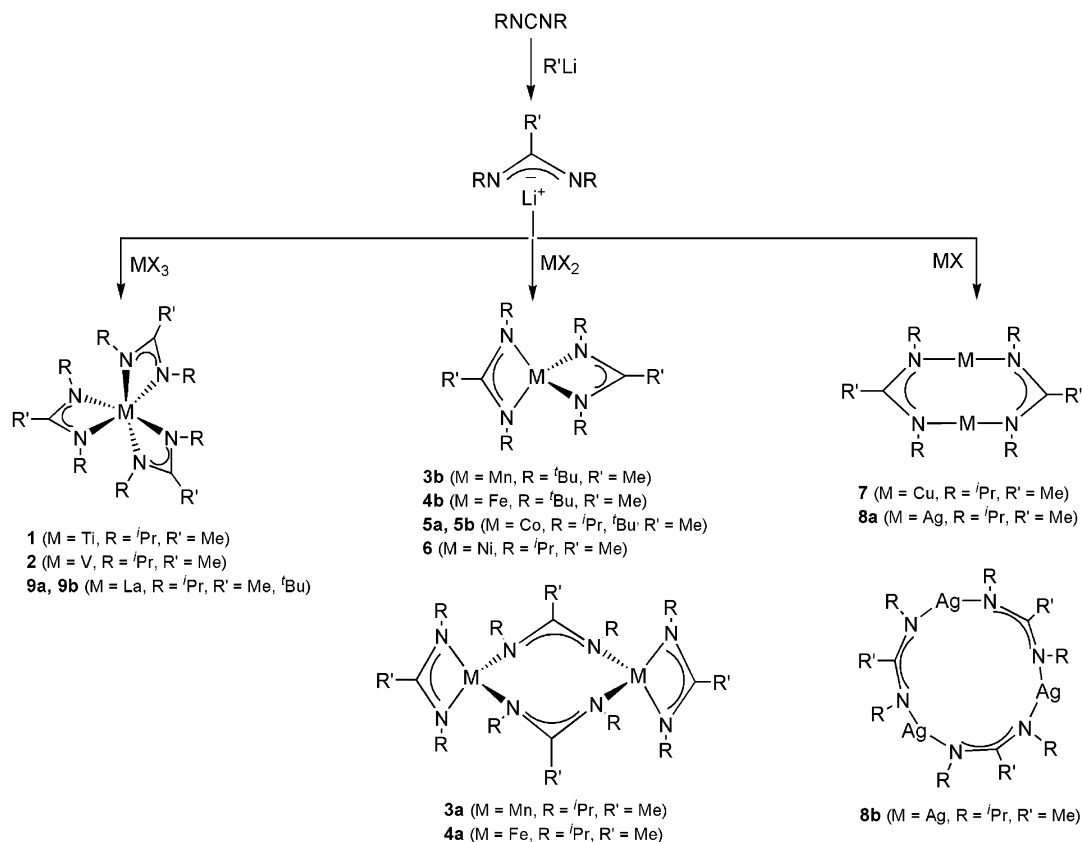
(a) Trivalent Metals. The acetamidinate ligand ⁱPr-MeAMD was utilized in the synthesis of Ti(III) and V(III) compounds. Dark brown titanium (**1**) and red-brown vanadium (**2**) compounds were obtained with 70% and 80% yields, respectively (Scheme 1). The ¹H NMR data and sublimation data supported the monomeric formulation for compounds **1** and **2** (Table 2). The structure of vanadium compound **2** is shown in Figure 2, and selected metric data

are collected in Table 3. Its structure was highly disordered over four positions, and only one position is shown in Figure 2 for the purpose of clarity. The molecule has a distorted geometry from octahedral toward trigonal prismatic with a N–V–N transoid angle of 163.9(7)° and a dihedral angle of $\theta = 85.9$ – 95.8° between VN₂ planes; its structure is similar to that observed in the analogous compound [V(*p*-tolyl)-HAMD]₃.¹⁸ The mean V–N bond distance is 2.02(2) Å, and the bite angle of the chelating η^2 -amidinate ligand is 63.5(6)°.

Unlike early transition metals, the tendency of lanthanide elements to acquire a coordination number higher than 3 is well-known, which often results in “ate” complexes possessing alkali-metal-bearing solvent molecules or one or two bridging halide anions.²⁷ For example, attempted synthesis of neutral homoleptic lanthanum compounds with diisopropylamide or 2,2,5,5-tetramethylpyrrolidinate (TMPR) ligands generated [La(NⁱPr₂)₂](μ -NⁱPr₂)₂[Li(THF)] and [La(TMPR)₃]₂-(μ -X)(M(THF)₄) (X = Cl, I, M = Li, Na), respectively.²⁸ With the more bulky 2,2,6,6-tetramethylpiperidinate (TMPD) ligand, we were able to synthesize successfully the neutral lanthanum compound [La(TMPD)₃].²⁹ This three-coordinate lanthanum compound was, however, thermally unstable, and decomposed at 138 °C. The strategy to increase the thermal stability of resultant compounds using the chelating bidentate ligands, ⁱPr-MeAMD and ⁱPr-^tBuAMD, finally led us to obtain thermally stable, neutral lanthanum compounds **9a** and **9b**, respectively, in good yields. A comparison of vapor

(27) Just, O.; Rees, W. S., Jr. *Inorg. Chem.* **2001**, *40*, 1751–1755 and references therein.

(28) (a) The compound [La(NⁱPr₂)₂](μ -NⁱPr₂)₂[Li(THF)] was prepared by the reaction of LaCl₃(THF)₂ with lithium diisopropylamide in THF. The compound crystallizes in monoclinic space group *P*2(1) with *a* = 15.26(1) Å, *b* = 21.43(2) Å, *c* = 21.47(2) Å, β = 95.251(8)°, *Z* = 2, and *V* = 6988(9) Å³. Flame test further confirmed the incorporation of lithium with this compound. Because this compound is not of direct interest in this work, it was not further characterized. (b) Compounds [La(TMPr)₃]₂(μ -X)[M(THF)₄] (X = Cl, I; M = Li, Na) were prepared by the reaction of LaX₃(THF)_n (X = Cl, *n* = 2, X = I, *n* = 4) with sodium or lithium salt of 2,2,5,5-tetramethylpyrrolidine (Lunt, E. *Tetrahedron Suppl.* **1963**, 291) in THF. One of these compounds, [La(TMPr)₃]₂(μ -I)[Na(THF)₄], crystallizes in monoclinic space group *P*2(1)/*c* with *a* = 11.04(1) Å, *b* = 27.81(2) Å, *c* = 24.25(2) Å, β = 94.32(2)°, *Z* = 4, and *V* = 7428(1) Å³. Silver nitrate experiments and flame test further confirmed the incorporation of halide and sodium or lithium, in these compounds, respectively. Because these compounds are not of direct interest in this work, they were not further characterized.

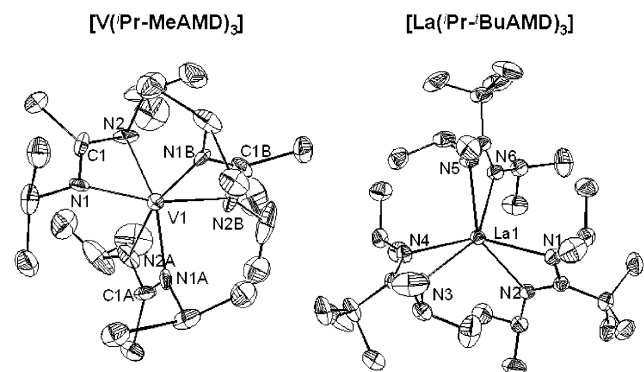
Scheme 1. Synthesis of Metal Amidinates

Table 3. Bond Distances (Å) and Angles (deg) for Trivalent Metal Amidinates **2** and **9b**

	2	9b
M–N ^a	2.06(4)	2.53(2)
N–C ^{a,b}	1.30(2)	1.332(3)
N–C–N ^b	114(2)	111.8(1)
N–M–N ^c	163.9(7)	149(2)
N–M–N ^{chelating} ^a	63.5(6)	51.8(2)
θ ^d	85.9, 93.3, 95.8	96.2, 98.7, 98.9

^a Mean values. ^b Amidinate backbone. ^c Transoid angle, involving N atoms in different chelate rings. ^d Dihedral angle between MN₂ planes.

Table 4. Vapor Pressures of Lanthanum(III) and Copper(I) Compounds with Various Amide-Type Ligands

compound	vapor pressure (°C/Torr)	refs
[La(TMS) ₃]	102/0.0001	11
[La(TMPD) ₃]	105/0.0001	this work
[La(ⁱ Pr- ^t BuAMD) ₃]	120/0.05	this work
[La(ⁱ Pr-MeAMD) ₃]	80/0.04	this work
[Cu(NEt ₂) ₄]	>90, dec	16
[Cu(TMS) ₄]	160/0.1	32
[Cu(TMPR) ₃]	100/0.04	this work
[Cu(ⁱ Pr-MeAMD) ₂]	70/0.05	this work


Figure 2. Structures of trivalent metal amidinate compounds **2** (left) and **9b** (right) showing 30% probability ellipsoids and partial atom-labeling schemes. Atoms labeled A and B are related to other atoms by C₃ symmetry.

pressures among homoleptic lanthanum compounds with amide-type ligands is summarized in Table 4. Lanthanum acetamidinate **9a** shows the highest volatility among them. Bidentate ⁱPr-MeAMD seems to have proper steric bulk for stabilizing ions both as big as lanthanum(III) and, at the same

time, as small as vanadium(III), generating six-coordinate compounds. The structure of **9b** is distorted trigonal prismatic with dihedral angles of θ = 96.2–98.9° and a mean N–La–N transoid angle of 149(2)° (Figure 2). The mean La–N bond length is 2.53(2) Å. The chelating η²-amidinate ligand in **9b** has a very small bite angle (N–M–N) of 51.8(2)°, as compared to that of the vanadium compound **2** (63.5(6)°). The geometry of the three La–N–C–N four-membered rings is essentially planar with a mean deviation from planarity of 0.0173–0.0473 Å.

(b) Divalent Metals. In the acetamidinate compounds of the divalent, first-row transition metals, the nitrogen atom substituents have a steric influence on the structures of the resulting metal compounds. Reactions of anhydrous MCl₂

(29) This compound was prepared by the reaction of LaCl₃(THF)₂ with lithium 2,2,6,6-tetramethylpiperidinate in THF. ¹H NMR (C₆D₆): 1.277 (m, 4H), 1.384 (s, 12H), 1.686 (m, 2H). It crystallizes in monoclinic space group P2(1)/n with a = 7.824(8) Å, b = 18.71(2) Å, c = 20.38(2) Å, β = 94.34(1)°, Z = 4, and V = 2975(5) Å³. With use of 7044 unique data, the structure was refined to R₁/wR₂ = 2.82/6.44%. Selected parameters: La–N, 2.363(1) Å; N–La–N, 120.0(4)°.

(M = Mn, Fe, Co, Ni) with 2 equivalents of *i*-Pr-MeAMD or *t*-Bu-MeAMD afforded dimeric [Mn₂(μ-*i*-Pr-MeAMD)₂(η²-*i*-Pr-MeAMD)₂] (**3a**) and [Fe₂(μ-*i*-Pr-MeAMD)₂(η²-*i*-Pr-MeAMD)₂] (**4a**) and monomeric compounds [Mn(*t*-Bu-MeAMD)₂] (**3b**), [Fe(*t*-Bu-MeAMD)₂] (**4b**), [Co(*i*-Pr-MeAMD)₂] (**5a**), [Co(*t*-Bu-MeAMD)₂] (**5b**), and [Ni(*i*-Pr-MeAMD)₂] (**6**). The assignment of solid structures for the compounds **3**–**6** was made on the basis of X-ray crystal structure determinations and/or molecular weight determination, ¹H NMR, sublimation, and elemental analysis data. It is notable that no lantern-type dinuclear compounds were formed in the case of acetamidinate ligands (*i*-Pr-MeAMD or *t*-Bu-MeAMD) unlike the earlier observation found in various metal compounds with aryl-substituted formamidinate ligands.^{18–20}

For the metals Mn(II) and Fe(II) with greater ionic size than that of Co(II) and Ni(II), the isopropyl substituents were not sufficient to provide monomeric structures, and generated dinuclear compounds containing two nonbridging and two bridging acetamidinate ligands. This behavior is similar to that reported for Mg(II) dimers bridged by *i*-Pr-MeAMD ligands.²⁴ The iron compound **4a** is dimeric in both solution and solid states, as confirmed by the molecular weight (complexity = 2.0(2)) and X-ray structure determinations. Although X-ray structure determination was not done for manganese compound **3a**, its similar sublimation temperature to that of the corresponding iron compound **4a** suggests that **3a** is also a dimer (Table 2). The structure of **4a** is shown in Figure 3, and selected bond distances and angles are contained in Table 5. The iron atoms are coordinated by both one η²-amidinate ligand and two bridging μ,η¹:η¹-amidinate ligands. The Fe–N distance of 2.112(1) Å in the bridging ligand is slightly longer than that observed in the terminal chelating ligand (2.074(5) Å). While the η²-amidinate ligand bound to Fe has a planar geometry with mean deviation of 0.0055 Å, the geometry of Fe–N–C–N–Fe containing the bridging amidinate ligands is not planar with an Fe–N–C–N dihedral angle of 62.5°. The relatively long Fe–Fe distance of 2.979(1) Å in **4a** as compared to 2.462 Å found in the lantern-type dimer [Fe(Ph-HAMD)₂]₂¹⁹ indicates that there is no iron–iron bond formation in this dimer; a similar observation was also made in the analogous compound [Fe₂(μ-Ph-PhAMD)₂(η²-Ph-PhAMD)₂]₂·2THF.¹⁹

In the case of Co(II) and Ni(II), the isopropyl groups are bulky enough to afford monomeric species. The nickel compound **6** is believed to be monomeric on the basis of the similarity of its ¹H NMR data and sublimation temperature to those of the related Co(II) compound **5a**, whose identity was confirmed by X-ray structure determination (Table 2, Figure 3). Molecular weight determination in *p*-xylene further showed that compound **6** is monomeric in solution; the determined complexity was 1.0(2). Introducing the larger *tert*-butyl groups in place of isopropyl groups in **3b**, **4b**, and **5b** prevents dimerization, affording monomeric species even for the larger Mn(II) and Fe(II) ions. This is again similar to the geometries reported for amidinate compounds of Mg.²⁴

The structures of monomeric compounds **4b** and **5a** are shown in Figure 3. Selected bond distances and angles are

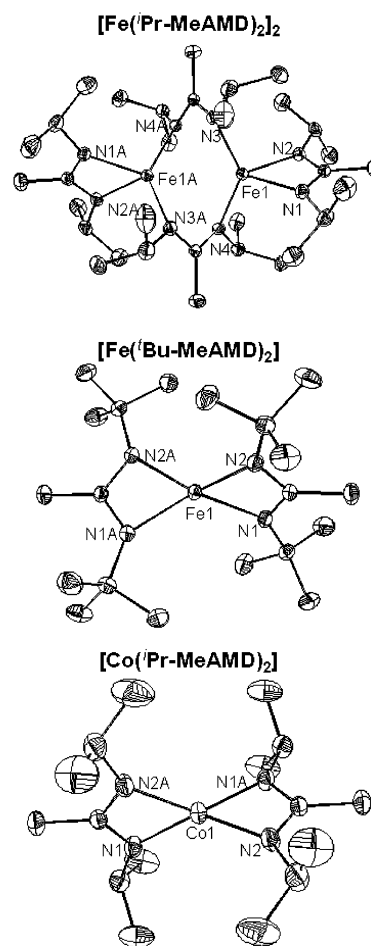


Figure 3. Structures of divalent metal amidinate compounds **4a** (top), **4b** (middle), and **5a** (bottom) showing 30% probability ellipsoids and partial atom-labeling schemes. Atoms labeled A are related to other atoms by C₂ symmetry (**4a**), mirror plane (**4b**), and C₂ symmetry (**5a**).

Table 5. Bond Distances (Å) and Angles (deg) for Divalent Metal Amidinates **4a**, **4b**, and **5a**

	4a	4b	5a
M–N ^a	2.074(5)	2.033(1)	2.012(8)
M–N _{bridging} ^a	2.112(1)		
N–C ^{a,b}	1.328(1)	1.337(1)	1.320(2)
N–C–N	113.1(2)	111.18(9)	111.2(2)
N–C–N _{bridging}	116.5(2)		
N–M–N	133.58(6)	139.72(7)	132.31(9)
	113.86(6)	127.78(4)	137.02(6)
	105.09(6)	146.54(7)	133.68(8)
	106.40(6)	127.78(4)	137.02(7)
	113.23(7)		
N–M–N _{chelating}	63.32(7)	65.52(4)	65.57(6)

^a Mean values. ^b Amidinate backbone.

given in Table 5. These compounds adopt a distorted tetrahedral environment around the metal center with two η²-amidinate ligands, which is similar to other reported compounds.^{19,23,24} The geometries of the M–N–C–N four-membered rings in both **4b** and **5a** are planar with an imposed mirror plane and C₂ symmetry, respectively. The mean M–N distances are 2.033(1) Å (**4b**) and 2.012(8) Å (**5a**), and the bite angles of amidinate ligand (N–M–N) are 65.52(4)° (**4b**) and 65.57(6)° (**5a**). Interestingly, the bite angle of 65.52(4)° in **4b** is very close to the value of the known [Fe(Cy-*t*-BuAMD)₂] (65.38(8)°).²³ Although comparison is imprecise because of differences in ligand system and

accuracy in X-ray structure determination, this observation indicates that the alkyl substituent on the carbon atom of the amidinate ligand from methyl group to *tert*-butyl group does not have a significant effect on the bite angles of the ligands in the resulting Fe(II) compounds.

Although tetrahydrofuran (THF) was used in the synthesis of **3–6**, THF adducts were not isolated, suggesting that the coordination of THF in these compounds is very weak or easily lost upon isolation. All the compounds **3–6** are paramagnetic as demonstrated by broad peaks in their ^1H NMR spectra.

(c) Monovalent Metals. Reaction of CuBr with 1 equiv of $^i\text{Pr-MeAMD}$ produced pale yellow solutions from which colorless copper compound **7** was isolated in 83% yield. When CuCl_2 was treated with 2 equiv of $^i\text{Pr-MeAMD}$, a redox reaction occurred instead of the expected metathesis reaction, generating the Cu(I) compound **7** in a quantitative yield. Similar redox chemistry caused by amide ligands has been previously shown.³⁰ The compound **7** turned out dimeric by the X-ray structure determination (Figure 4). The dimeric unit in **7** is the smallest unit among known homoleptic Cu(I) amide-type compounds. Known examples of $[\text{Cu}(\text{NR}_2)]_4$ and $[\text{Cu}(\text{TMS})]_4$ are tetrameric, and the compound with TMPR ligand is trimer $[\text{Cu}(\text{TMPR})]_3$, whose identity was confirmed by X-ray structure determination.³¹ Because of its small molecular weight, dimeric **7** showed the highest volatility among the Cu(I) amide compounds, as summarized in Table 4.

In a similar way, but with AgCl, silver compound **8** was also prepared in 90% yield. While the copper compound **7** is dimeric in both solution and solid states, the corresponding silver compound **8** exists as a mixture of dimer and trimer in a 1:1 (mol/mol) ratio in solution at room temperature and in a 1:2 (mol/mol) ratio in the solid state, as accessed by ^1H NMR spectroscopy and by X-ray structure determination (Figure 4). Attempts to separate the dimeric form from the mixture by sublimation at 80 °C under 40 mTorr gave a 1:1 mixture of dimer and trimer after sublimation. This observation suggests that the sublimed dimer quickly equilibrated to a dimer/trimer mixture on the coldfinger or in benzene solution during the NMR measurement. A relatively low melting point of 95 °C was observed for the mixture of silver compounds (**8a**, **8b**).

Structures of the copper (**7**) and silver compounds (**8a**, **8b**) are shown in Figure 4, and selected bond lengths and angles are collected in Table 6. The compound **7** is a dimer in the solid state in which acetamidinate ligands bridge copper atoms in a $\mu, \eta^1: \eta^1$ -fashion. The average Cu–N distance is 1.869(1) Å, and this distance is quite similar to

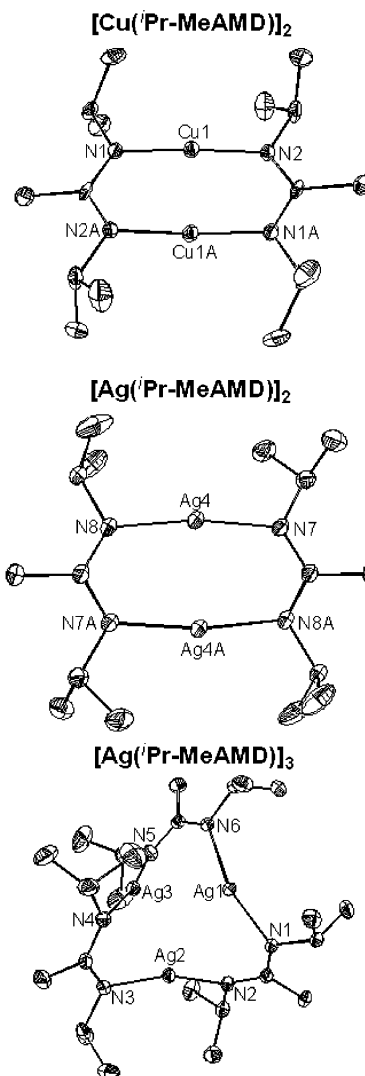


Figure 4. Structures of monovalent metal amidinate compounds **7** (top), **8a** (middle), and **8b** (bottom) showing 30% probability ellipsoids and partial atom-labeling schemes. Atoms labeled A are related to other atoms by an inversion center.

Table 6. Bond Distances (Å) and Angles (deg) for Monovalent Metal Amidinates **7**, **8a**, and **8b**

	7	8a	8b
M–N ^a	1.869(1)	2.111(3)	2.12(2)
N–C ^{a,b}	1.329(2)	1.331(5)	1.328(4)
M–M ^a	2.414(1)	2.645(1)	2.99(2)
N–C–N ^b	120.0(7)	121.4(3)	119.0(7)
N–M–N ^a	176.4(1)	170.8(1)	164(3)

^a Mean values. ^b Amidinate backbone.

that observed in the analogous compound $[\text{Cu}(p\text{-tolyl-HAMD})]_2$ (1.87(1) Å).²⁰ The geometry of the silver compound **8a** is very close to that of the corresponding copper compound **7**. Again, the Ag–N distance of 2.111(3) Å is similar to that observed in $[\text{Ag}(p\text{-tolyl-HAMD})]_2$ (1.87(1) Å).²⁰ The distances between metal atoms in these dimers are 2.414(1) Å in **7** and 2.645 Å in **8a**, indicating the presence of some metal–metal interaction. The geometries of the M–N–C–N–M in **7** and **8a** are planar with imposed centrosymmetry, and N–M–N are essentially linear with 176.4(1)° and 170.8(1)°, respectively. In the trimeric silver

(30) Tayebani, M.; Kasani, A.; Feghali, K.; Gambarotta, S.; Bensimon, C. *Chem. Commun.* **1997**, 2001–2002 and references therein.

(31) This compound was prepared by the reaction of CuCl with lithium 2,2,5,5-tetramethylpyrrolidinate in Et₂O. ^1H NMR (C₆D₆): 1.548 (s, 12H), 1.671 (s, 4H). It crystallizes in hexagonal space group P6(3)/m with $a = 10.219$ (6) Å, $b = 10.219$ (6) Å, $c = 14.48$ (1) Å, $Z = 6$, and $V = 1309$ (2) Å³. With use of 1039 unique data, the structure was refined to $R_1/wR_2 = 3.73/9.83\%$. Selected parameters: Cu–N, 1.93–(1) Å; Cu–Cu, 2.471(2) Å; Cu–N–Cu, 79.6(1)°; N–Cu–N, 160.4–(1)°.

(32) Baxter, D.; Chisholm, M. H. *Chem. Vap. Deposition* **1995**, 1, 49.

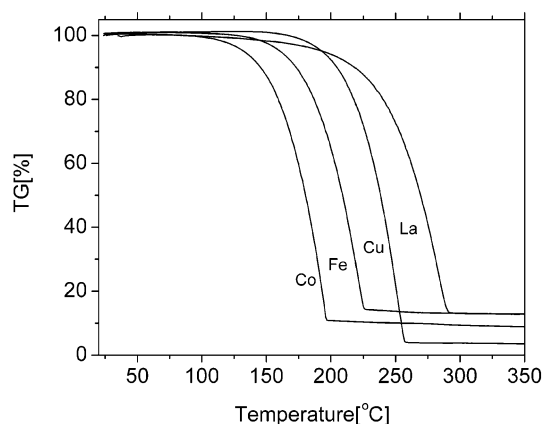


Figure 5. TG curves for mass changes of acetamidinate compounds of iron (**4b**), cobalt (**5a**), copper (**7**), and lanthanum (**9a**) measured in a nitrogen flow at atmospheric pressure.

compound **8b**, the amidinate ligands are bridging three silver atoms in a $\mu, \eta^1: \eta^1$ -fashion as depicted in Figure 4. The mean Ag–N distance of 2.12(2) Å in this trimer is essentially the same as that observed in the dimer **8a**.

Utility as Precursors for ALD. Finding effective ALD precursors is difficult because they must meet several very stringent requirements: (1) sufficient volatility (>about 0.1 Torr); (2) sufficient thermal stability (>months at vaporization temperature, >seconds at deposition temperature); (3) high but self-limited reactivity with surfaces prepared by a complementary reactant and also with suitably prepared substrates; (4) saturation thickness independent of the flux of molecules to the surfaces; (5) saturated surface suitable for reaction with a complementary precursor.

As our initial goal of preparing these metal amidinate compounds is to use them as precursors for ALD, we examined the volatility and thermal stability of compounds **1–9**. No decomposition was observed during sublimation, showing that the compounds are stable at the sublimation temperatures listed in Table 2. These precursors are all volatile enough for use in ALD with the precursor vapor sources held at temperatures below 120 °C. TGA/DSC measurements of the manganese (**3b**), iron (**4b**), cobalt (**5a**), nickel (**6**), copper (**7**), and lanthanum (**9a**) acetamidinates at atmospheric pressure were also performed. Representative TGA curves are given in Figure 5. Vaporization occurs cleanly in one step with low residual mass (**3b** left 4%, **4b** left 12%, **5a** left 9%, **7** left 1%, **9a** left 12%), except for the nickel compound **6**, which had a step suggesting decomposition at about 180 °C and a higher residual mass (27%). This suggests that the compounds are thermally stable during vaporization even at a pressure as high as 1 atm. The only features in most of the DSC curves (not shown) were endothermic peaks due to the melting and evaporation of the compounds, which further demonstrates their thermal stabilities. Only **6** (Ni) showed an exothermic peak in its DSC, indicating decomposition at 180 °C. The TGA/DSC studies demonstrate the stability of the compounds for minutes at temperatures above 200–250 °C (the maximum measurement temperature being limited by the vaporization

of the samples). Thermal stability for short times (≤ 1 s) at higher temperatures was determined by flowing the vapors (entrained in N_2) through a tube furnace, and noting the lowest temperature at which material is deposited on a heated substrate in the tube. The resulting decomposition temperatures are the following: **3b** (Mn) 300 °C, **4b** (Fe) 300 °C; **5a** (Co) 350 °C; **6** (Ni) 300 °C; **7** (Cu) 300 °C; **9a** (La) 350 °C. In order to preserve self-limited reactivity in ALD processes using these precursors, the substrate temperatures must be kept below these values.

We recently showed that **4b**, **5a**, **6**, and **7** could be used for ALD of pure Fe, Co, Ni, and Cu thin films, respectively, using hydrogen as the second precursor.²⁵ When water vapor was used in place of hydrogen as the complementary reactant, metal oxide films such as FeO, CoO, and La_2O_3 were deposited. Because of their high reactivity with oxygen and water vapor, these compounds must be carefully protected from contact with ambient atmosphere. The nitrogen carrier gas must also be purified to remove traces of oxygen and moisture, which interfere with the ALD processes.

Compounds **1–9** are successful as ALD precursors; they are sufficiently volatile, thermally stable, and highly reactive. The high volatility is achieved because the outer regions of the molecules are largely hydrocarbon, leading to weak interactions between the molecules. The volatility is also enhanced by the low nuclearity of the structures (mostly monomeric) enforced by the bulky ligands. This lack of oligomerization also allows them to vaporize rapidly even from the solid state. They are highly soluble in hydrocarbon solvents, so direct liquid injection of their solutions is also a convenient method for vaporizing them. The chelating effect of the amidinate ligands contributes to the high thermal stability of the compounds. Despite this high thermal stability, the compounds are highly reactive, in part because the order of the metal–nitrogen bonds is only one-half. Their high reactivity under ALD conditions is shown by the nearly complete removal of the ligands, which results in low impurity levels of the deposited films, as demonstrated in ALD of pure Fe, Co, Ni, Cu, FeO, CoO, and La_2O_3 thin films.²⁵ Another attractive feature of the metal amidinates is that they do not contain halides, which can contaminate films or corrode apparatus. Furthermore, amidinates are very versatile ligands, forming a series of compounds with metals having a wide range of sizes from V(III) to La(III) and oxidation states 1, 2, and 3.

Acknowledgment. We thank Ms. Ying Wang for assistance in the preparation of 2,2,5,5-tetramethylpyrrolidine and $[La(TMPD)_3]$. We appreciate the TGA/DSC analyses provided by Dr. Xinjian Lei of Schumacher, a unit of Air Products. This work was supported in part by the National Science Foundation (Grant No. ECS 9975504).

Supporting Information Available: X-ray crystallographic files in CIF format for the structure determinations of the eight compounds in Table 1. This material is available free of charge via the Internet at <http://pubs.acs.org>.

IC0345424